



**HAL**  
open science

## Observation of the dynamics of polyelectrolyte strong solutions by quasi-elastic neutron scattering

F. Nallet, G. Jannink, J.B. Hayter, R. Oberthür, C. Picot

► **To cite this version:**

F. Nallet, G. Jannink, J.B. Hayter, R. Oberthür, C. Picot. Observation of the dynamics of polyelectrolyte strong solutions by quasi-elastic neutron scattering. *Journal de Physique*, 1983, 44 (1), pp.87-99. 10.1051/jphys:0198300440108700 . jpa-00209577

**HAL Id: jpa-00209577**

**<https://hal.science/jpa-00209577>**

Submitted on 4 Feb 2008

**HAL** is a multi-disciplinary open access archive for the deposit and dissemination of scientific research documents, whether they are published or not. The documents may come from teaching and research institutions in France or abroad, or from public or private research centers.

L'archive ouverte pluridisciplinaire **HAL**, est destinée au dépôt et à la diffusion de documents scientifiques de niveau recherche, publiés ou non, émanant des établissements d'enseignement et de recherche français ou étrangers, des laboratoires publics ou privés.

Classification  
Physics Abstracts  
61.40K

## Observation of the dynamics of polyelectrolyte strong solutions by quasi-elastic neutron scattering

F. Nallet, G. Jannink, J. B. Hayter (\*), R. Oberthür (\*) and C. Picot (\*\*)

SPSRM, Orme des Merisiers, 91191 Gif sur Yvette Cedex, France

(Reçu le 10 juin 1982, révisé le 13 septembre, accepté le 28 septembre 1982)

**Résumé.** — Des expériences de diffusion quasi élastique de neutrons, dont nous présentons les résultats, ont été réalisées sur des solutions aqueuses concentrées de polyélectrolytes, sans sel. Le polyion est du polystyrène sulfoné associé successivement à des contreions sodium et tétraméthylammonium. Dans ce dernier cas, nous avons étudié toutes les combinaisons possibles de polyions et contreions deutérés et non deutérés.

Les grandeurs extraites des données expérimentales sont tout d'abord les facteurs de structure statique des polyions et des contreions. Les contributions cohérentes et incohérentes au facteur de structure dynamique sont ensuite séparées. Le coefficient d'autodiffusion des contreions est alors déterminé à partir de la diffusion incohérente. Un coefficient de diffusion dépendant du vecteur d'onde est obtenu à partir de la diffusion cohérente. Ce coefficient est lié au mode lent du processus collectif de relaxation. Nous trouvons que la mobilité associée à ce mode est une fonction du vecteur d'onde, ce qui répond à une question soulevée auparavant à propos du facteur de structure dynamique d'un polyélectrolyte flexible. Nous n'avons pas réussi à observer le mode rapide du processus de relaxation, malgré l'utilisation des différentes combinaisons de polyions et contreions marqués.

**Abstract.** — We report results of quasi-elastic neutron scattering experiments on concentrated polyelectrolyte solutions in water without added salt. The polyion is sulphonated polystyrene, associated successively with sodium and tetramethylammonium counterions. In this second case, all possible configurations of deuterated and non deuterated charged components are tested.

The quantities first derived from the experiment are the static polyion and counterion structure factors. Next, the coherent and incoherent contributions to the time-dependent structure factors are separated. The counterion self diffusion coefficient is determined from the incoherent scattering. A wave-dependent diffusion coefficient is derived from the coherent scattering. This coefficient is associated with the slow collective relaxation mode. The mobility related to this mode is found to have a characteristic wavevector dependence, settling thereby a question raised earlier about the dynamic structure factor of polyelectrolytes made of flexible coils. The attempt to observe the fast relaxation mode using the different labelled combinations failed.

**1. Introduction.** — Polyelectrolytes are multicomponent systems made of large polyions and small counterions dissolved in a polar solvent. Thermal agitation induces characteristic mass and charge fluctuations. Two dissipative processes control the concentration fluctuations [1, 2]. The first is mass diffusion along a concentration gradient; the second is convection due to electric fields arising from these gradients. Their combined effects yield characteristic variations of transport coefficients, such as molecular mobility, with the parameters of the solution. It is of

general interest to study these variations experimentally, since the effect of the Coulomb interaction on the observable properties of the system is difficult to account for in an explicit manner through rigorous, statistical mechanical calculations. Other static or transport properties of polyelectrolyte solutions not yet thoroughly theoretically understood, are, for instance, the existence of a maximum value of the polyion-polyion partial static structure factor at some transfer wavevector  $q_m$  varying as  $c^{1/2}$  [3], or the anomalous value of the electrical conductivity [4]. They are also attributed to the strong Coulomb couplings. Here we consider the time and space dependence of the concentration autocorrelation functions. Unlike the case of ordinary diffusive behaviour, two characteristic relaxation frequencies are expected to

(\*) ILL, 156X, Centre de tri, 38042 Grenoble Cedex, France.

(\*\*) CRM, 6, rue Boussingault, 67083 Strasbourg Cedex, France.

be found, with one non zero relaxation frequency at zero transfer wavevector. The dissymmetry in mass and charge between polyions and counterions, typical of a polyelectrolyte, produces other specific dynamic properties. When the polyion is a rigid molecule, as is the case with polystyrene latex, the dynamics of the system can be in some respect treated in a simplified way, using the Born-Oppenheimer hypothesis. The counterion equilibration time [2] is small compared to the corresponding polyion time and, as a consequence, the two species can be considered separately. When the polyion is made of long, flexible coils, as is the case in this report, the dissymmetry is still large but its effect is tempered, in concentrated solutions, because of the overlapping of the coils. Here the elementary time for the polyion is fixed by the size of the rigid units associated with the random coil configuration. But the main fact of interest in this case is that the polyion concentration fluctuations have long-range spatial correlations, which are sensitive to molecular interactions, and whose variations can be measured over a large  $q$  range from a scattering experiment. The characteristic variation with  $q$  of the time-dependent pair correlation functions serves as a test for the formulation of the dynamic properties in such systems.

In a preceding letter [5], a problem was raised concerning the  $q$ -dependence of the effective diffusion coefficient,  $D(q)$ , related to the polyion concentration fluctuations. The data published in reference [5] suggested that  $D(q)$  probably changes from a decreasing to a *constant* function of  $q$  as  $q$  increases beyond  $q_m$ . However, there was not enough experimental material to settle the matter conclusively. We thus performed more neutron quasi-elastic scattering experiments at the Institut Laue-Langevin (Grenoble). Our results, reported here, allow, hopefully, a definite conclusion to be drawn. Moreover, as the possible influence of counterions on the polyelectrolyte solution dynamics was not previously investigated, we tried to point out this influence. To this end, experiments were carried out on all possible combinations of labelling the polyion-counterion system. In principle, this allows us to make both a clearer distinction between coherent and incoherent scattering and a separate evaluation of the contribution to coherent scattering of each mode that might exist in our coupled, three-component system. In particular, the so-called « plasmon » mode should become observable. Unfortunately, we were not able to reach that goal, and the question about counterions remains unanswered.

Subsequent parts are organized as follows :

- Part 2 : Neutron scattering cross-sections ;
- Part 3 : Samples ;
- Part 4 : Instrument description and performances ;
- Part 5 : Results ;
- Part 6 : Theoretical considerations ;
- Part 7 : Discussion of the results.

**2. Neutron scattering cross-sections.** — A neutron scattering experiment is, basically, the measurement

of an intensity  $I(\mathbf{q}, \omega)$  as a function of the transfer wavevector  $\mathbf{q}$  and the energy transfer  $\hbar\omega$ . Assuming single collisions, the general expression for  $I(\mathbf{q}, \omega)$  is [6] :

$$I(\mathbf{q}, \omega) = K \left[ \sum_{I,J} a_I a_J S_{IJ\text{coh}}(\mathbf{q}, \omega) + \sum_I \frac{\sigma_I}{4\pi} S_{I\text{inc}}(\mathbf{q}, \omega) \right] \quad (1)$$

$K$  is an apparatus constant, the indices  $I$  and  $J$  run over all the components of the system (in our case three components, the solvent  $I = 0$ , the polyion  $I = 1$  and the counterion  $I = 2$ ). The transfer wavevector  $\mathbf{q}$  is related to the scattering angle  $\theta$ , the energy transfer  $\hbar\omega$  and the wavelength  $\lambda$  of the scattered neutrons. In the quasi-elastic approximation ( $\hbar\omega$  smaller than the neutron incident energy) we have :

$$q = |\mathbf{q}| = \frac{4\pi}{\lambda} \sin \frac{\theta}{2}.$$

The coherent dynamic scattering function  $S_{IJ\text{coh}}(\mathbf{q}, \omega)$  is defined by [6] :

$$S_{IJ\text{coh}}(\mathbf{q}, \omega) = \int_{-\infty}^{+\infty} e^{i\omega t} \left\langle \sum_{i \in I, j \in J} e^{i\mathbf{q} \cdot (\mathbf{r}_i(t) - \mathbf{r}_j(0))} \right\rangle dt \quad (2)$$

and the incoherent dynamic scattering function  $S_{I\text{inc}}(\mathbf{q}, \omega)$  by [6] :

$$S_{I\text{inc}}(\mathbf{q}, \omega) = \int_{-\infty}^{+\infty} e^{i\omega t} \left\langle \sum_{i \in I} e^{i\mathbf{q} \cdot (\mathbf{r}_i(t) - \mathbf{r}_i(0))} \right\rangle dt \quad (3)$$

that is, as time Fourier transforms of the intermediate scattering functions, respectively  $F_{IJ\text{coh}}(\mathbf{q}, t)$  and  $F_{I\text{inc}}(\mathbf{q}, t)$ .  $\mathbf{r}_{Ii}(t)$  is the position, at time  $t$ , of the  $i$ th elementary scatterer belonging to component  $I$ ; such an elementary scatterer is chosen so as to have a negligible size as compared to  $q^{-1}$  (i.e. a constant form factor), and is here the solvent molecule ( $I = 0$ ), the polyion monomer ( $I = 1$ ) or the counterion ( $I = 2$ ).  $a_I$  and  $\sigma_I$  are respectively the coherent scattering length and the incoherent cross-section of the elementary scatterer of the  $I$ th component.

The quantities  $F_{IJ\text{coh}}(\mathbf{q}, t)$  and  $F_{I\text{inc}}(\mathbf{q}, t)$ , which may be expressed, in the quasi-elastic approximation, as inverse Fourier transforms :

$$F_{IJ\text{coh}}(\mathbf{q}, t) = \frac{1}{2\pi} \int_{-\infty}^{+\infty} e^{-i\omega t} S_{IJ\text{coh}}(\mathbf{q}, \omega) d\omega \quad (4)$$

$$F_{I\text{inc}}(\mathbf{q}, t) = \frac{1}{2\pi} \int_{-\infty}^{+\infty} e^{-i\omega t} S_{I\text{inc}}(\mathbf{q}, \omega) d\omega \quad (5)$$

are of great interest because they are directly measured with one of the spectrometers used in our experiments (see Part 4). Moreover,  $F_{IJ\text{coh}}(\mathbf{q}, t = 0) \equiv S_{IJ\text{coh}}(\mathbf{q})$  is the partial  $IJ$  coherent static scattering function.

Because of the long-range correlations in polyelectrolyte solutions (polymer structure and electric interactions), small-angle scattering experiments are interesting. In this  $q$  range, the incompressibility constraint has to be taken into account; this is done later (see Part 6).

A characteristic of the neutron scattering experiment, as compared to light scattering for instance, is apparent in the  $I(\mathbf{q}, \omega)$  formula (1). The self transport properties of the system are encoded in the incoherent contributions (3) to the total intensity and must be separated from the collective ones (2).

It is possible to modify, to a large extent, the coherent scattering lengths of some species in the system by labelling them without altering chemical properties. This is accomplished for instance by substituting deuterium nuclei to the protons of some scattering units. This possibility is of great importance for at least two reasons. The separate evaluation of coherent and incoherent contributions is feasible, as is the identification of each mode of collective behaviour that a multicomponent system may exhibit. This only requires a proper « tuning » of the  $a_i$ 's (see Part 6).

**3. Sample description.** — The samples are sodium and tetramethylammonium polystyrene sulphonates (PSSNa, PSSTMA).

Working with wholly deuterated or non deuterated polyion, or counterion, various combinations may be obtained. We used : PSS<sub>H</sub>Na, PSS<sub>H</sub>TMA<sub>H</sub>, PSS<sub>H</sub>TMA<sub>D</sub>, PSS<sub>D</sub>TMA<sub>D</sub>, PSS<sub>D</sub>TMA<sub>H</sub>. (The index H or D indicates a hydrogenated or deuterated molecule.)

In the case of the PSSTMA samples, the styrene polymerization and the sulphonation were carried out at the Centre de Recherches sur les Macromolécules (CRM) (Strasbourg). The (weight-average) degree of polymerization of the parent polystyrenes (hydrogenated and deuterated) is  $N_w = 1\,200$ . The Vink method [7] was used for both sulphonations. There is about 90 % or more sulphonated styrene per chain, and the polydispersity of the samples after sulphonation is known through the ratio  $N_w/N_n$ , equal to 1.25 in the best case and to 1.40 in the worst.

The PSS<sub>H</sub>Na sample was bought from the Pressure Chemical Company (Pittsburg). The (weight-average) index of polymerization is  $N_w = 950$ . All the samples were dialyzed against pure water.

The solvent is pure heavy water (D<sub>2</sub>O) <sup>(1)</sup>; no salt is added.

Concentrations are evaluated from measured solvent volume and solute mass before mixing, using the tabulated partial molar volumes of PSSTMA and PSSNa [8].

<sup>(1)</sup> We have used the D<sub>2</sub>O obtained from the Département des Molécules Marquées, CENS, without further purification.

In the case of PSSNa, the solute concentration  $C$  is :  
 $c = 350$  monomole. $\cdot$ m<sup>-3</sup> ( $c = 7.21 \times 10^{-2}$  g. $\cdot$ cm<sup>-3</sup>),  
and in the case of PSSTMA :

$$c = 590 \text{ monomole} \cdot \text{m}^{-3} \quad (c = 1.6 \times 10^{-1} \text{ g} \cdot \text{cm}^{-3}).$$

In order to check the validity of these values, we measured the mass density of the PSS<sub>H</sub>TMA<sub>H</sub> and PSS<sub>H</sub>TMA<sub>D</sub> with the high-precision digital densitometer [9]. The results

$$\rho_{\text{HH}} = 1.124\,4 \text{ g} \cdot \text{cm}^{-3}$$

and

$$\rho_{\text{HD}} = 1.128\,8 \text{ g} \cdot \text{cm}^{-3}$$

are consistent with the values derived above, i.e.

$$\frac{\rho_{\text{measured}} - \rho_{\text{calculated}}}{\rho_{\text{measured}}} \simeq 0.5 \%.$$

In this range of concentration, the strong solute-solute correlations are reflected by the existence of a maximum in the coherent polyion-polyion scattering function (see Ref. [3]).

According to this reference, the peak position is  $q_m = 1.2$  nm<sup>-1</sup> (PSSNa), and, from interpolation of the  $q_m(c)$  law,  $q_m = 1.3$  nm<sup>-1</sup> for the PSSTMA's. The temperature is room temperature for PSSTMA and 25 °C for PSSNa. The Debye screening length  $\kappa^{-1}$  calculated from the number of counterions assuming full dissociation is :

$$\kappa^{-1} = \begin{cases} 0.71 \text{ nm (PSSNa)} \\ 0.55 \text{ nm (PSSTMA)}. \end{cases}$$

The main interest in using labelled species for neutron scattering experiments comes from the possibility of adjusting the effective scattering length to a useful value. Values are given in table I of the incoherent

Table I. — Neutron coherent scattering and contrast lengths for the components of the polyelectrolyte solution.  $a_1$  coherent scattering length,  $v_1$  partial molar volume,  $b_1$  contrast length,  $\sigma_1$  incoherent scattering cross-section, for the elementary scatterer of component I.

	PSS monomer		TMA		Na	D <sub>2</sub> O
	H	D	H	D		
$a_1$ 10 <sup>-12</sup> cm	4.72	12.0	- 0.89	11.6	0.36	1.91
$v_1$ cm <sup>3</sup> · mol <sup>-1</sup>	114	114	84	84	- 6.6	18
$b_1$ 10 <sup>-12</sup> cm	- 7.40	- 0.11	- 9.28	2.67	1.06	0
$(\sigma_1/4\pi)^{1/2}$ 10 <sup>-12</sup> cm	6.67	1.15	8.73	1.49	0.38	0.60

scattering cross-section  $\sigma_I$ , the coherent scattering length  $a_I$ , and the contrast length  $b_I = a_I - \frac{v_I}{v_0} a_0$  for the molecule monomers of component  $I$  (i.e. PSS<sup>-</sup>, TMA<sup>+</sup> or Na<sup>+</sup>). The quantity  $v$  is the partial volume of the species, and index 0 refers to the solvent (D<sub>2</sub>O). Notice that in this case the incoherent scattering cross-section is accounted for mostly by spin incoherence (and not by isotopic incoherence).

**4. Spectrometer description.** — The spin-echo (IN11) and the back-scattering (IN10) spectrometers of the Institut Laue-Langevin were used in this experiment. They are described in detail in references [10, 11, 12]. It is however useful to define here the quantities measured from these instruments.

The spin-echo spectrometer gives as final output the normalized intermediate scattering function

$$F_N(q, t) = \frac{F(q, t)}{F(q, 0)}. \quad (6)$$

This quantity is obtained from a succession of elementary measurements, which we describe below assuming an ideal, fully efficient apparatus. IN11 is a two-axis spectrometer for which the incident neutron beam is polarized (all spins « up »). Along the two arms, a magnetic guide field is kept uniform and constant. At the beginning of the first arm and at the end of the second one, a  $\pi/2$  spin-turn coil is placed. Between the two arms, near the sample, there is a  $\pi$  spin-turn coil.

An experimental configuration is defined by :

- a scattering angle  $\theta$
  - a guide field value  $B$  (the time in  $F(q, t)$  is actually proportional to  $B$ )
  - a state of the spin-turn coils : « on » or « off ».
- Moreover when the second  $\pi/2$  coil is « on », its current may be either positive or negative.

The neutron detector is placed behind the polarization analyser. Given an experimental configuration, the measured quantity is the scattered neutron flux with spin « up ».

Let  $I_+$  ( $I_-$ ) be the flux when all spin-turn coils are on, with a positive (negative) current in the second  $\pi/2$  coil;  $I^\uparrow$  the flux when all spin-turn coils are off and  $I^\downarrow$  the flux when all but the  $\pi$  spin-turn coils are off. It is shown (see Ref. [12]) that, if the isotopic incoherence is negligible, the following relations hold :

$$I^\uparrow \sim I_{\text{coh}}(\mathbf{q}) + \frac{1}{3} I_{\text{inc}}(\mathbf{q})$$

$$I^\downarrow \sim \frac{2}{3} I_{\text{inc}}(\mathbf{q})$$

$$I_\pm \sim I_{\text{coh}}(\mathbf{q}) + I_{\text{inc}}(\mathbf{q}) \mp [I_{\text{coh}}(\mathbf{q}, t) - \frac{1}{3} I_{\text{inc}}(\mathbf{q}, t)]$$

with

$$I_{\text{coh}}(\mathbf{q}, t) = \sum_{I, J} a_I a_J F_{IJ\text{coh}}(\mathbf{q}, t)$$

$$I_{\text{inc}}(\mathbf{q}, t) = \frac{1}{4\pi} \sum_I \sigma_I F_{I\text{inc}}(\mathbf{q}, t)$$

and

$$I_{\text{coh}}(\mathbf{q}) = I_{\text{coh}}(\mathbf{q}, 0), \quad I_{\text{inc}}(\mathbf{q}) \equiv I_{\text{inc}}(\mathbf{q}, 0).$$

Thus with our ideal spectrometer,  $F_N(\mathbf{q}, t)$ , defined as

$$F_N(\mathbf{q}, t) = \frac{I_{\text{coh}}(\mathbf{q}, t) - \frac{1}{3} I_{\text{inc}}(\mathbf{q}, t)}{I_{\text{coh}}(\mathbf{q}, 0) - \frac{1}{3} I_{\text{inc}}(\mathbf{q}, 0)}$$

is given by

$$F_N(\mathbf{q}, t) = \frac{I_- - I_+}{I^\uparrow - I^\downarrow} \quad (7)$$

and the relative weight of coherent scattering

$$y = \frac{I_{\text{coh}}(\mathbf{q})}{I_{\text{coh}}(\mathbf{q}) + I_{\text{inc}}(\mathbf{q})}$$

by :

$$y = \frac{I^\uparrow - \frac{1}{2} I^\downarrow}{I^\uparrow + I^\downarrow}. \quad (8)$$

The discussion is slightly more complicated for the real spectrometer. Nevertheless the basic ideas, and the IN11 performances, remain very similar.

The available scattering angles range from  $\theta = 2^\circ$  to  $\theta = 20^\circ$ . For our experiment (choice of the guide field  $B$ ) the minimum value of the time is  $t_m = 0.5$  ns with a maximum one  $t_M = 10.7$  ns. The mean wavelength is  $\lambda = 0.83$  nm, with a 8% relative spread (mechanical velocity selector). The accessible transfer wavevectors  $q$  and transfer energies  $\omega$  are then, respectively :

$$0.2 \text{ nm}^{-1} \leq q \leq 1.8 \text{ nm}^{-1}$$

$$30 \text{ neV} \leq \omega \leq 200 \text{ neV}.$$

The back-scattering spectrometer, IN10, measures an  $M(\mathbf{q}, \omega)$  obtained by the convolution of the intensity  $I(\mathbf{q}, \omega)$  (form. 1) with a resolution function  $G_\theta(\omega)$ .  $M(\mathbf{q}, \omega)$  is observed for seven values of  $\theta$ , between  $4^\circ$  and  $17.8^\circ$ , with  $\omega$  ranging from  $-12 \mu\text{eV}$  to  $+12 \mu\text{eV}$  by steps of  $0.2 \mu\text{eV}$ . The width of the resolution function is always about  $1.8 \mu\text{eV}$ . The incident, Bragg reflected, neutrons have a wavelength  $\lambda = 0.628$  nm. This leads to a reciprocal space domain

$$0.7 \text{ nm}^{-1} \leq q \leq 3.1 \text{ nm}^{-1}.$$

We now describe and compare the IN10 and IN11 data processing :

IN10 :

We choose *a priori* an analytical form for the  $\omega$  dependence of  $I(\mathbf{q}, \omega)$  within the three following possibilities :

—  $I(\mathbf{q}, \omega)$  is a Lorentzian, characterized by four parameters : background, i.e.  $\lim_{\omega \rightarrow \infty} I(\mathbf{q}, \omega)$ ; position, i.e. value  $\omega_0$  at the maximum of  $I(\mathbf{q}, \omega)$ ; height, i.e.  $I(\mathbf{q}, \omega_0)$ ; half width at half maximum.

—  $I(\mathbf{q}, \omega)$  is the sum of two Lorentzians centred at the same point : six parameters.

—  $I(\mathbf{q}, \omega)$  is the sum of a Lorentzian and of a delta function, centred at the same point : five parameters.

The chosen  $I(\mathbf{q}, \omega)$  is then numerically convoluted with the experimental  $G_\theta(\omega)$  and the result fitted, varying all the parameters and according to a least squares criterion, to the experimental  $M(\mathbf{q}, \omega)$ .

IN11 :

In this case a *time* convolution analysis is also necessary, in principle. But in practice there is no need for such a sophistication. According to the IN11 time scale, we are studying rather slowly-varying phenomena. The width of the time resolution function is much less than the relaxation times of our  $F_N(\mathbf{q}, t)$ , and it is therefore legitimate to factor out of the convolution integral. Hence, IN10 results are less reliable and less easily interpreted than those obtained with IN11.

5. Results. — 5.1 STATIC STRUCTURE FACTORS. —

As a check, the coherent static intensity  $I_{\text{coh}}(\mathbf{q})$  was measured, using IN11, for all the samples. When the polyion is the more luminous component of the solution (hydrogenated polyion with sodium or deuterated TMA) the characteristic polyelectrolyte static structure factor is seen, with a position of the interaction peak in rough agreement with the results of reference [3] (Fig. 1). In this case :

$$I_{\text{coh}}(\mathbf{q}) \approx b_1^2 S_{11\text{coh}}(\mathbf{q}).$$

On the other hand, if the polyion is deuterated its contrast length is nearly zero (Table I); the intensity recorded thus comes entirely from the counterions and only the partial counterion-counterion coherent static scattering function is observed (Fig. 1) :

$$I_{\text{coh}}(\mathbf{q}) \approx b_2^2 S_{22\text{coh}}(\mathbf{q}).$$

Also obtained by this static polarization analysis is the identification, in the scattered intensity, of the coherent and incoherent scattering contributions.

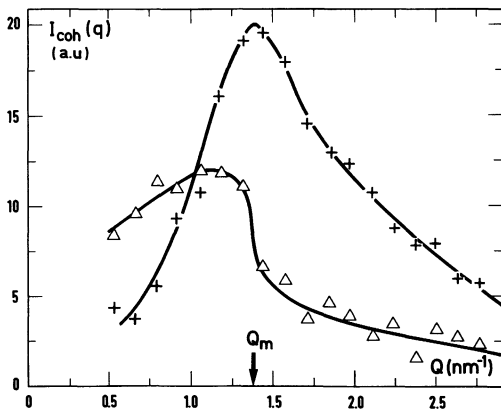


Fig. 1. — Polyion-polyion (+) and counterion-counterion (Δ) scattering functions, directly obtained from the elastic scattering experiments : + PSS<sub>H</sub>TMA<sub>D</sub>; Δ PSS<sub>D</sub>TMA<sub>H</sub>.

Results are displayed on figure 2 where

$$\frac{I_{\text{coh}}(\mathbf{q})}{I_{\text{coh}}(\mathbf{q}) + I_{\text{inc}}(\mathbf{q})}$$

is plotted against  $q$  for the four PSSTMA samples. It is worth mentioning that the wholly-deuterated sample, PSS<sub>D</sub>TMA<sub>D</sub>, which gives an acceptable coherent level relative to the incoherent one, is actually a bad choice because of its overall very low intensity in D<sub>2</sub>O.

5.2 DYNAMIC STRUCTURE FACTORS. — 5.2.1 IN11.

— The normalized intermediate scattering function  $F_N(\mathbf{q}, t)$  is obtained with the PSS<sub>H</sub>Na and PSS<sub>H</sub>TMA<sub>H</sub> samples. Measurements are made at 8 values of the scattering angle  $\theta$ , namely  $\theta = 4, 5, 6, 8, 10, 11, 12$ , and 15 degrees, with PSS<sub>H</sub>Na, but only at 2 values  $\theta = 7^\circ$  and  $\theta = 15^\circ$  with PSS<sub>H</sub>TMA<sub>H</sub>. Figure 3 shows a representative spectrum. Though the data acquisition duration of such a spectrum is about one day,

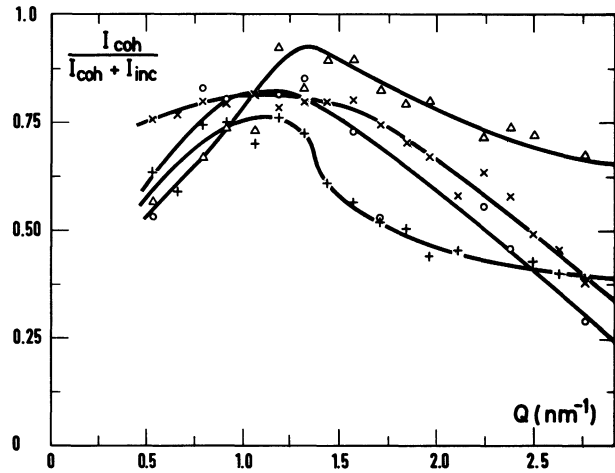


Fig. 2. — Ratio of coherent intensity to total intensity (static measurements) : ○ PSS<sub>D</sub>TMA<sub>D</sub>; Δ PSS<sub>H</sub>TMA<sub>D</sub>; + PSS<sub>D</sub>TMA<sub>H</sub>; × PSS<sub>H</sub>TMA<sub>H</sub>.

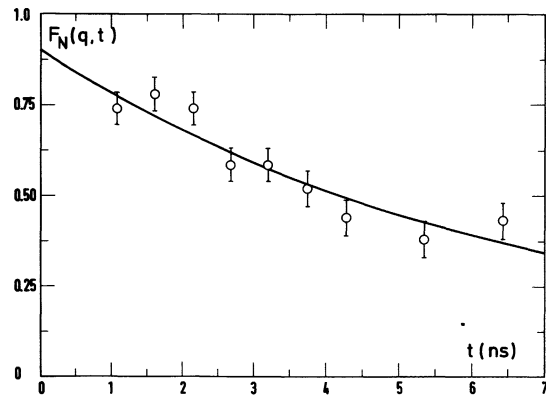


Fig. 3. — Normalized intermediate scattering function  $F_N(q, t)$  for PSS<sub>H</sub>Na at  $q = 1.58 \text{ nm}^{-1}$ ; continuous curve : fitted  $A e^{-t/\tau}$ .

the precision of our measurements is rather poor : this exemplifies the low luminosity of polyelectrolytes dissolved in pure water. We did not try to use elaborate data analysis methods, like cumulant expansions, etc., to represent these spectra.

If we assume that  $F_N(\mathbf{q}, t)$  is the sum of several relaxation modes we have :

$$F_N(\mathbf{q}, t) = \frac{\sum A_i(\mathbf{q}) e^{-t/\tau_i(\mathbf{q})}}{\sum A_i(\mathbf{q})} \quad (F_N(\mathbf{q}, 0) = 1).$$

In the long-time limit, all but the slowest mode have decayed to zero, hence :

$$F_N(\mathbf{q}, t) \simeq \frac{A_s(\mathbf{q}) e^{-t/\tau_s(\mathbf{q})}}{\sum A_i(\mathbf{q})} \quad (9)$$

where  $\tau_s$  is the characteristic relaxation time of this mode.

This long-time limit is no longer normalized to unity when extrapolated back to  $t = 0$  : the normalization is a short-time property and here we study explicitly the long-time behaviour. We thus restricted ourselves to a (two-parameter) fit of  $F_N(\mathbf{q}, t)$  by a single decaying exponential :  $F_N(\mathbf{q}, t) = A e^{-t/\tau}$ . This allows us to define a ( $q$ -dependent) relaxation frequency  $\tau^{-1}$ , characteristic of the slow mode. Figure 4 shows the dispersion relation  $\tau^{-1}(q)$  for the PSS<sub>H</sub>Na sample. An important related quantity is easily obtained : the effective,  $q$ -dependent, diffusion coefficient  $D(q) = \frac{\tau^{-1}}{q^2}$ . A curve of  $D(q)$  is drawn on figure 5.

The different behaviour for  $q < q_m$  and for  $q > q_m$  is easily seen on this plot. The (approximately) constant value of the effective diffusion coefficient at large  $q$  is about  $D \simeq 6.0 \times 10^{-11} \text{ m}^2 \cdot \text{s}^{-1}$ .

5.2.2 IN10. — The quantity  $M(\mathbf{q}, \omega)$  is measured for the four PSSTMA samples. Two functions  $M(\mathbf{q}, \omega)$

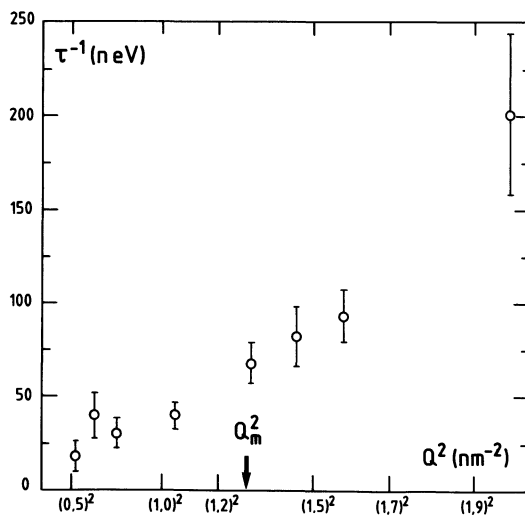


Fig. 4. — Dispersion relation  $\tau_s^{-1}(q^2)$  for the PSS<sub>H</sub>Na sample.

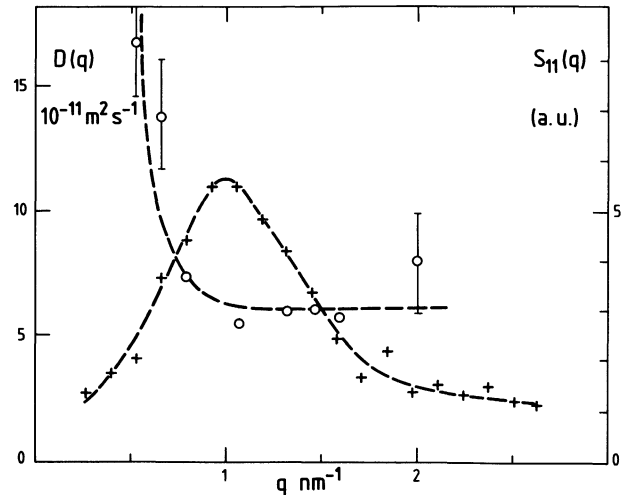


Fig. 5. — Effective diffusion coefficient  $D(q)$  (○) and polyion-polyion structure factor  $S_{11}(q)$  (+), for the PSS<sub>H</sub>Na sample. The dashed lines are only eye guides.

at fixed  $\theta = 8.6^\circ$  ( $q = 1.5 \text{ nm}^{-1}$ ) are shown in figure 6. In the first case the sample is vanadium ; its dynamic scattering function is seen as an incoherent elastic peak :  $I(\mathbf{q}, \omega) \sim \delta(\omega)$ . Thus the curve is the resolution function  $G_\theta(\omega)$ . In the second case the sample is PSS<sub>H</sub>TMA<sub>H</sub>. The spectra are reduced to the same height, to facilitate the comparison between the apparatus and sample broadenings. The second curve is not centred around  $\omega = 0$ , because the resolution function is not a symmetric function about the origin. As is apparent in figure 6, the convolution analysis is necessary to recover the sample true  $I(\mathbf{q}, \omega)$ ; therefore the data were analysed according to the methods described in § 4.

From the study of the PSS<sub>D</sub>TMA<sub>H</sub> sample, the polarization analysis establishes that incoherent scattering is important at large  $q$  values and almost as important as coherent scattering at small  $q$ 's (see Fig. 2).

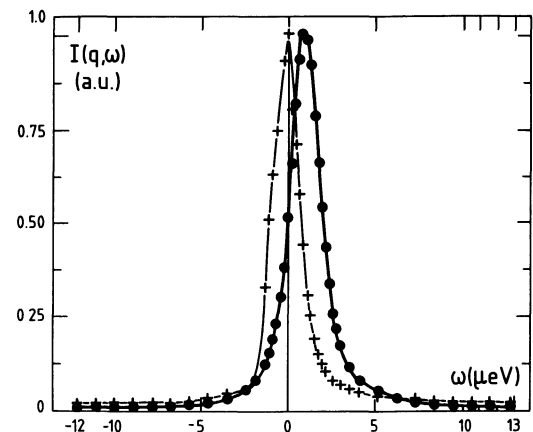


Fig. 6. — IN10 raw spectra  $M(q, \omega)$ ,  $q = 1.5 \text{ nm}^{-1}$ . + resolution function ; ● PSS<sub>H</sub>TMA<sub>H</sub> sample. The resolution width is  $1.8 \mu\text{eV}$  and the sample broadening is  $2.2 \mu\text{eV}$ .

At small  $q$ 's the best representation of  $I(\mathbf{q}, \omega)$  is the sum of an elastic peak and a Lorentzian. At large  $q$ 's the data are best fitted with one Lorentzian. Its broadening  $\gamma$  thus originates from incoherent scattering. A linear relationship between  $\gamma$  and  $q^2$  is observed (Fig. 7). The measured diffusion coefficient, defined by  $D = \gamma q^{-2}$ , is  $D = 3.7 \times 10^{-10} \text{ m}^2 \cdot \text{s}^{-1}$ .

In the whole  $q$  range probed, the  $\text{PSS}_\text{H}\text{TMA}_\text{D}$  intensity is mostly coherent, excluding perhaps the first point (Fig. 2). At the four last angles, it is possible to fit a single broadened Lorentzian to the experimental data. In this high- $q$  limit, the broadening  $\gamma$  is again linear in  $q^2$  (Fig. 8). We have thus a well-defined diffusion coefficient  $D = 1 \times 10^{-11} \text{ m}^2 \cdot \text{s}^{-1}$ . Results are not altogether satisfying because none of the three possible representations of  $I(\mathbf{q}, \omega)$  is acceptable for the first three scattering angles. The numerical fit leads to « unphysical » broadenings for  $I(\mathbf{q}, \omega)$  less than the  $\omega$  step value ( $\sim 0.2 \mu\text{eV}$ ). The actual broadenings are too small to be measured using this spectrometer.

The situation is similar for the  $\text{PSS}_\text{H}\text{TMA}_\text{H}$  sample. At all but the last two points the intensity is coherent. No fit is physically reliable at small angles for the same reason as given above. At large angles, a fit using two broadened Lorentzians gives the best result. Nevertheless, the broadening  $\Gamma$  of the broader Lorentzian, which could be identified with a fast mode relaxation frequency, has a rather chaotic  $q$  behaviour, probably because  $\Gamma$  is near the upper  $\omega$ -space limit:  $\Gamma \sim 6\text{-}8 \mu\text{eV}$ . The broadening  $\gamma$  of the other Lorentzian is also of the form  $\gamma = Dq^2$ , with nearly the same diffusion coefficient as defined with  $\text{PSS}_\text{H}\text{TMA}_\text{D}$  (Fig. 9). Two complementary measurements were made on  $\text{PSS}_\text{H}\text{TMA}_\text{H}$  with IN11. The relaxation frequencies measured are also on the curve  $\gamma = Dq^2$ . The same mode is observed with the two spectrometers.

No results could be obtained with the wholly-deuterated sample  $\text{PSS}_\text{D}\text{TMA}_\text{D}$ , not luminous enough to give us confidence in the numerical deconvolution analysis.

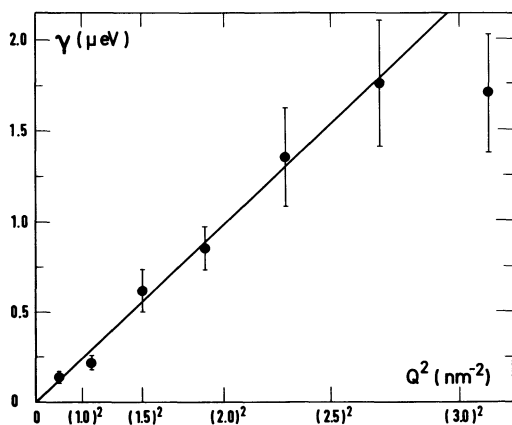


Fig. 7. — Dispersion relation  $\gamma(q^2)$  for the  $\text{PSS}_\text{D}\text{TMA}_\text{H}$  sample. The straight line is the least squares fit passing through the origin.

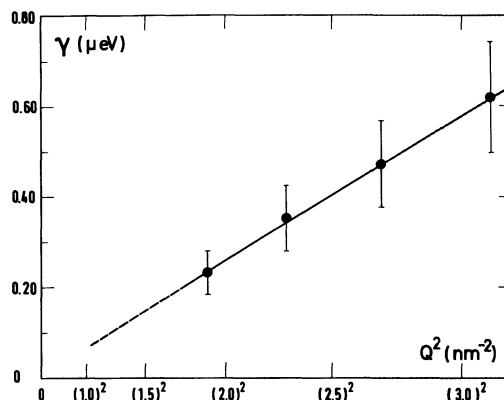


Fig. 8. — Dispersion relation  $\gamma(q^2)$  for the  $\text{PSS}_\text{H}\text{TMA}_\text{D}$  sample.

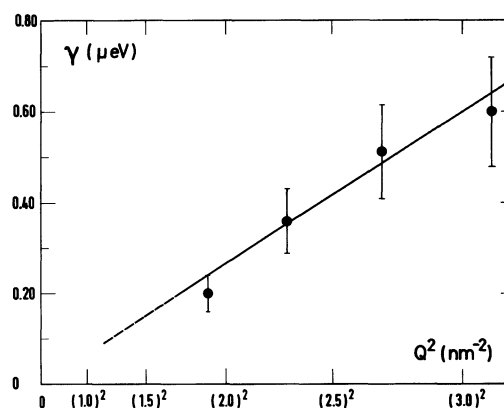


Fig. 9. — Dispersion relation  $\gamma(q^2)$  for the  $\text{PSS}_\text{H}\text{TMA}_\text{H}$  sample.

**6. Theoretical considerations.** — In this part, we present theoretical models designed to describe some essential features of the dynamics of charged systems. The theoretical approach to the dynamics of polyelectrolyte solutions is difficult because both polymer and electrolyte properties should be taken into account. The electrolyte character brings in strong and long-range electrical interactions. On the other hand, the polymer chain has many internal degrees of freedom and there are specific intra- and interchain correlations. Models expounded in the following are therefore often not satisfactory because they emphasize either the electrolyte or the chain properties. But they are nevertheless useful for their qualitative predictions.

Theoretical calculations consist in transforming the basic expressions for the cross-sections, given in Part 3, into function of collective or self-transport coefficients. We examine the results of such calculations successively for the incoherent and the coherent contribution. The experimental evaluation was discussed in the preceding section.

6.1 THE INCOHERENT CONTRIBUTION : SELF DIFFUSION MOTION. — The following model deals with the self diffusion of the counterions in a polyelectrolyte solution and allows us to compute the counterion incoherent dynamic scattering function,  $S_{2,inc}(\mathbf{q}, \omega)$ . The small ions are subject to a rapid brownian motion in the electric field created by the large, and therefore slowly moving, polyions. The resulting effect of this electrical interaction is a slowing down of the diffusive motion of the counterions. Picturesquely, we may say that the counterion spends more time moving against the electric field than it does moving with it. The relation between the self diffusion coefficient of the counterion in the polyelectrolyte solution,  $D_2$ , and the one it would have in a very dilute solution with small ions as a substitute for polyions,  $D_2^0$ , is [13] :

$$D_2 = fD_2^0$$

where  $f$  is a function, always smaller than unity, of the Manning dimensionless « condensation » parameter  $l_B/a$ , where  $l_B$  is the Bjerrum length of the solvent,  $l_B = \frac{e^2}{4\pi\epsilon_0\epsilon_r kT}$ , and  $a$  the spacing between charged groups on the polyion chain. It should be noted that, although the « condensation » parameter appears in the calculation, the slowing down of the diffusive motion of the counterions basically originates from the Coulomb interaction and not from the so called « counterion condensation » [14] :  $f < 1$  even if no « condensation » occurs (i.e.  $f < 1$  even if  $l_B/a < 1$ ).

We apply this result to the incoherent counterion intermediate scattering function; its relaxation frequency will be :  $\tau^{-1} = D_2 q^2 = fD_2^0 q^2$ , which gives a measurement of this  $f$  factor at the microscopic scale probed by neutron scattering.

The scattering experiment by the PSS<sub>D</sub>TMA<sub>H</sub> sample provides us with a good check for this calculation. As seen in Part 5, the intensity scattered by this sample is mostly incoherent and the hydrogenated counterion is the more efficient scatterer. The curve displayed in figure 7 is the counterion self diffusion motion dispersion relation.

Our value for the self diffusion coefficient of tetramethylammonium counterion in a semi-dilute polyelectrolyte solution, deduced from the dispersion curve, is :  $D_2 = 3.7 \times 10^{-10} \text{ m}^2 \cdot \text{s}^{-1}$ . A tabulated value, for TMA in a very dilute simple electrolyte solution is [15] :  $D_2^0 = 1.19 \times 10^{-9} \text{ m}^2 \cdot \text{s}^{-1}$ . The Manning  $f$  factor is thus here  $f = 0.3$ . Manning's theoretical calculations give  $f_{th} = 0.28$ , and conductivity measurements yield  $f_{exp} = 0.32$  [16]. This value is derived from observations on dilute sodium polystyrene sulphonates. The agreement with our result may therefore be only fortuitous.

6.2 THE COHERENT CONTRIBUTION : CONCENTRATION FLUCTUATIONS. — In the concentration range where the polyion chains overlap with neighbours the coherent dynamic functions  $S_{JJ,coh}(q, \omega)$  are related to the collective diffusive motions of the species. This rela-

tionship can be derived from equations for the time and space dependence of concentration fluctuations.

Such equations have a simple structure when only linear terms in concentration fluctuations are retained and when the (macro) molecules are treated as structureless particles. It is then possible to account for some essential features of the concentration autocorrelation function, but not for the specific dynamic behaviour of polyelectrolytes made of long, flexible coils. In a previous report [5] these formal results were modified to include a wavevector dependent mobility  $\mu(\mathbf{q})$ , introduced to account for the internal structure and for the small-scale rigidity of a polyelectrolyte chain.

The coherent dynamic functions  $S_{JJ}(\mathbf{q}, \omega)$  are given here using first the simplified theory (structureless particles) and then according to reference [5]. The simplified theory is expected to be valid only in the small- $q$  domain. Its interest is that it explicitly considers all the components, solvent, counterion and polyion on a par, and thus provides a convenient framework within which to discuss the influence of the counterions on collective dynamical properties. To our knowledge there is no such framework for the higher- $q$  regime. That is why we reproduce below the arguments given before in reference [5], to cope with high- $q$  situations.

As seen in Part 2 we have to calculate, for example, the following intensity

$$I(\mathbf{q}, t) = \sum_{I,J} a_I a_J \left\langle \sum_{i \in I} \sum_{j \in J} e^{i\mathbf{q} \cdot (\mathbf{r}_i(t) - \mathbf{r}_j(0))} \right\rangle_{eq} \quad (10)$$

where  $\langle \dots \rangle_{eq}$  is an average over the equilibrium initial distribution. We define the concentration  $\hat{c}_I$  of the « elementary units » of component  $I$  as

$$\hat{c}_I(\mathbf{r}, t) = \sum_{i \in I} \delta(\mathbf{r} - \mathbf{r}_i(t))$$

and the fluctuation  $\delta\hat{c}_I$  as

$$\delta\hat{c}_I(\mathbf{r}, t) = \hat{c}_I(\mathbf{r}, t) - \langle \hat{c}_I(\mathbf{r}, t) \rangle_{eq}$$

$\langle \hat{c}_I(\mathbf{r}, t) \rangle_{eq}$  is the usual, thermodynamic concentration,  $c_I$ .

In terms of spatial Fourier transforms, we have for  $q \neq 0$

$$I(\mathbf{q}, t) = \sum_{IJ} a_I a_J \langle \delta\hat{c}_I^*(\mathbf{q}, 0) \delta\hat{c}_J(\mathbf{q}, t) \rangle_{eq} \quad (11)$$

We now use the Onsager's regression hypothesis to set

$$\langle \delta\hat{c}_I^*(\mathbf{q}, 0) \delta\hat{c}_J(\mathbf{q}, t) \rangle_{eq} = \overline{\delta\hat{c}_I^*(\mathbf{q}, 0) \delta\hat{c}_J(\mathbf{q}, t)}$$

where  $\delta c_J(\mathbf{q}, t) \equiv \langle \delta\hat{c}_J(\mathbf{q}, t) \rangle$  is the average of  $\delta\hat{c}_J(\mathbf{q}, t)$  over a non-equilibrium initial distribution, and changes with time according to macroscopic transport equations, such as the hydrodynamic ones. This determines  $\delta c_J(\mathbf{q}, t)$  as a function of the initial conditions  $\delta c_K(\mathbf{q}, 0)$ . Formally :

$$\delta c_J(\mathbf{q}, t) = C_J[\delta c_K(\mathbf{q}, 0); \mathbf{q}, t].$$

The average  $\overline{\dots}$  is defined as :

$$\overline{\delta c_I^*(\mathbf{q}, 0) \delta c_J(\mathbf{q}, t)} = \langle \delta c_I^*(\mathbf{q}, 0) C_J[\delta \hat{c}_K(\mathbf{q}, 0); \mathbf{q}, t] \rangle_{\text{eq.}}$$

The two major couplings controlling the relaxation processes are the overall incompressibility constraint and the electric interaction between charged components. We therefore write the transport equations as an incompressibility relation :

$$v_0 \delta c_0(\mathbf{q}, t) + v_1 \delta c_1(\mathbf{q}, t) + v_2 \delta c_2(\mathbf{q}, t) = 0 \quad (12)$$

( $v_I$  partial volume of the  $I$ th species) and as continuity equations for the two solute components

$$\partial_t \delta c_I(\mathbf{q}, t) = -i\mathbf{q} \cdot \mathbf{j}_I(\mathbf{q}, t) \quad (I = 1, 2) \quad (13)$$

where the current  $\mathbf{j}_I(\mathbf{q}, t)$  is assumed to be the sum of a diffusion term,  $\mathbf{j}_{I,d}$ , obeying Fick's law

$$\mathbf{j}_{I,d} = -iD_I \mathbf{q} \delta c_I,$$

and of a convection term  $\mathbf{j}_{I,c}$ , accounting for the coupling between the two solute components [1, 2]. The coupling is itself due to the electric field created by the concentration fluctuations. This contribution is essentially non linear. However it is evaluated as a linear combination of concentration fluctuations

$$\mathbf{j}_{I,c} = \sum_K \mathbf{l}_{IK} c_K.$$

This may be thought of as the first-order term of an expansion for the « true » current. It neglects also all thermal or viscous couplings.

The equations of motion for the solute components are of the general form

$$\partial_t \delta c_I = \sum_K A_{IK} \delta c_K$$

and are easily solved. In matrix notations

$$\delta c(\mathbf{q}, t) = e^{A(\mathbf{q})t} \delta c(\mathbf{q}, 0).$$

The expression for the intermediate scattering function, using the incompressibility relation, becomes

$$I(\mathbf{q}, t) = \sum_{IJ} \left( a_I - \frac{v_I}{v_0} a_0 \right) \left( a_J - \frac{v_J}{v_0} a_0 \right) \times \overline{\delta c_I^*(\mathbf{q}, 0) \delta c_J(\mathbf{q}, t)}$$

or  $I(\mathbf{q}, t) = B^+ Q B$ , where  $B$  is the contrast length column vector :

$$B = (b_I)_{I=1,2}, \quad b_I = a_I - \frac{v_I}{v_0} a_0$$

and  $Q$  is the quadratic form :

$$Q = (Q_{IJ}) \\ Q_{IJ} = \frac{1}{2} \left[ \overline{\delta c_I^*(\mathbf{q}, 0) \delta c_J(\mathbf{q}, t)} + \overline{\delta c_J^*(\mathbf{q}, 0) \delta c_I(\mathbf{q}, t)} \right]$$

or

$$Q_{IJ} = \frac{1}{2} [\sum_K S_{IK}(\mathbf{q}) (e^{A(\mathbf{q})t})_{JK} + S_{JK}(\mathbf{q}) (e^{A(\mathbf{q})t})_{IK}]$$

( $S_{IJ}(\mathbf{q}) = \langle \delta c_I^*(\mathbf{q}, 0) \delta c_J(\mathbf{q}, 0) \rangle_{\text{eq}}$  is the  $I$ - $J$  partial static scattering function).

Before giving more explicit results, we must remark that our calculation method, based on Onsager's hypothesis and on phenomenological transport equations, may sometimes not be self consistent. The scattering cross-section is always positive but our method does not retain this property, unless special conditions are met. Easily worked out is the following necessary condition (2 × 2 case) :

$$A_{11}(\mathbf{q}) S_{21}(\mathbf{q}) - A_{22}(\mathbf{q}) S_{12}(\mathbf{q}) = S_{11}(\mathbf{q}) A_{21}(\mathbf{q}) - S_{22}(\mathbf{q}) A_{12}(\mathbf{q}).$$

Other necessary conditions appear as inequalities and are less important constraints. In the subsequent general discussion we shall assume that the dynamic matrix  $A(\mathbf{q})$  is chosen to be compatible with the cross-section positivity requirement.

Diagonalizing the (two by two) matrix  $A(\mathbf{q})$ , we find a two-mode structure of  $I(\mathbf{q}, t)$  :

$$I(\mathbf{q}, t) = S(\mathbf{q}) e^{-t/\tau_s} + \mathcal{F}(\mathbf{q}) e^{-t/\tau_f} \quad (14)$$

where  $\tau_s^{-1}$  (resp.  $\tau_f^{-1}$ ) is the relaxation frequency of the slow (resp. fast) mode ( $\tau_s^{-1} < \tau_f^{-1}$ ) and  $S, \mathcal{F}$  are amplitudes depending on the contrast lengths  $b_I$ , on the  $S_{IJ}$ , and on the matrix elements  $A_{IJ}(\mathbf{q})$ . Their explicit form is not particularly illuminating (see Appendix A). The relaxation frequencies  $\tau^{-1}$  lead to  $q$ -dependent effective diffusion coefficients  $D_{\text{eff}} = \tau^{-1} q^{-2}$ .

The motions are strongly coupled in the sense that even if, say,  $b_1 = 0$ , neither  $S(\mathbf{q})$  nor  $\mathcal{F}(\mathbf{q})$  is in general zero. But at large  $q$  values (i.e. when looking for small spatial scale behaviour) decoupling occurs and the two components act as if independent :

$$\tau_s^{-1}(q) \sim D_1 q^2, \quad \tau_f^{-1}(q) \sim D_2 q^2.$$

(If we suppose, for example, that the  $I = 1$  component is the larger and therefore less mobile one :  $D_1 < D_2$ .) These are very general features of any coupled two-component system. When the solute components are charged, the electrical-neutrality condition introduces a constraint and new features emerge. The fast mode becomes a (non-propagating) « plasmon » mode, i.e.  $\tau_f^{-1}(0_+) > 0$  (usually  $\tau_f^{-1}(0_+) = \tau_s^{-1}(0_+) = 0$ ) and  $\mathcal{F}(0_+)$  is identically zero.

Explicit expressions may be given within the model of Berne and Pecora [2], which describes the dynamics of an electrolyte solution made of rigid molecules. Let  $D_-$  and  $D_+$  be the self diffusion coefficients respectively for the anion and the cation. Using our preceding notation (see Eq. 13),  $D_+ = D_2$ . Let  $z$  be the charge ratio between anion and cation. The dyna-

mic matrix is in this case

$$A(\mathbf{q}) = -D_+ \kappa^2 \begin{bmatrix} \left(z + \frac{q^2}{\kappa^2}\right) \frac{D_-}{D_+} & -\frac{D_-}{D_+} \\ -z & \left(1 + \frac{q^2}{\kappa^2}\right) \end{bmatrix} \quad (15)$$

where  $\kappa^{-1}$  is the Debye screening length.

This form for the dynamic matrix is consistent with the cross-section positivity requirement, for small  $q$ 's, because of the electroneutrality conditions :

$$zS_{11}(0_+) = S_{12}(0_+); \quad zS_{12}(0_+) = S_{22}(0_+).$$

(see Appendix B).

The slow and fast mode relaxation frequencies are easily obtained. In the small- $q$  limit :

$$\begin{aligned} \tau_f^{-1} &= (zD_- + D_+) K^2 + 0(q^2); \\ \tau_s^{-1} &= \frac{(z+1)D_- D_+}{zD_- + D_+} q^2 + 0(q^4) \end{aligned} \quad (16)$$

for large wavevector  $q$  values :

$$\tau_f^{-1} \simeq D_+ q^2, \quad \tau_s^{-1} \simeq D_- q^2. \quad (17)$$

Moreover, the following inequalities hold true

$$\tau_f^{-1} > D_+ q^2 > \tau_s^{-1}, \quad \text{if } D_+ > D_-.$$

In order to interpret our experimental data, we may first use the Berne and Pecora model defined above, and thus neglect the coil-like structure. For this, we need to define the « anion » which best describes the dynamics of our polyelectrolytes using the above equations. Because the coils are flexible, the « anion » is a unit whose size ranges from the entire coil to the monomer. The blob of size  $\xi = \kappa^{-1}$  (Debye screening length) was proposed to be such a unit [17-19]. In this case, the self diffusion coefficient  $D_-$  is the coefficient corresponding to the blob of size  $\xi$ . Expressions (16) and (17) can then be used to determine the time dependences in (14). Our final, qualitative, results are then : a two-mode structure of  $I(q, t)$ , with a (low intensity) plasmon mode; a diffusion coefficient associated with the slow mode which exhibits plainly, for small  $q$ 's, the coupling between polyions and counterions. It is a decreasing function of  $q$  and becomes a property of the sole polyion for large  $q$ 's.

An improvement for such a model, as regards the polyion dynamics, is then found by acknowledging the internal structure of the coil; this is done in reference [5]. Counterions are ignored for large  $q$ 's; according to the simplified analysis made above this should cause no harm.

The essence of the analysis given in reference [5] is to consider that the measured signal  $I(q, t)$  reduces, for high enough  $q$  values, to :

$$I(q, t) = b_1^2 S_{11}(q) e^{-D(q)q^2 t},$$

with the following structure for the  $q$ -dependent effective diffusion coefficient  $D(q)$  :

$$D(q) = kT \frac{\mu(q)}{S_{11}(q)}.$$

Such a formulation is very general and not restricted to polyelectrolyte systems. It may formally be obtained by linear response theory [21], which, however, does not explicitly give the mobility  $\mu(q)$ . In reference [5] the theoretical prediction for the behaviour of the mobility  $\mu$  as a function of  $q$  is :

$$\mu(q) = \mu(l_p^{-1}) (ql_p)^{-1} \quad \text{for } q > l_p^{-1}$$

where  $l_p$  is the persistence length of the polyelectrolyte chain [20]. Since the authors in [5] assume the following  $q$ -dependence for  $S_{11}(q)$  :

—  $S_{11}(q)$  increases roughly linearly with  $q$  in the range  $l_p^{-1} < q < q_m$  (rod-like behaviour with important interchain effects).

—  $S_{11}(q)$  behaves as  $q^{-1}$  for  $q > q_m$  (pure rod-like behaviour without interference between chains), their prediction for the law  $D(q)$  is :  $D(q)$  decreases rapidly (as  $q^{-2}$ ) for  $l_p^{-1} < q < q_m$  and  $D(q)$  becomes constant for  $q > q_m$ .

With the data recorded on the IN10 and IN11 spectrometers, it is now possible to discuss these theoretical predictions about the (theoretically primary) quantity  $\mu(q)$  and the (experimentally primary) quantity  $D(q)$ . The link between the two quantities will be the experimentally-determined  $S_{11}(q)$  and *not*, as in reference [5], a model for this polyion scattering function.

## 7. Discussion of the results. — 7.1 IN11 STATICS. —

Using the various  $PSS_{H,D}$  polyions and  $TMA_{H,D}$  counterions in  $D_2O$ , the polyion-polyion and counterion-counterion partial static scattering functions are directly derived from the elastic scattering data. The classic results are obtained. A perhaps interesting continuation of such studies using properly-chosen combinations of deuterated and hydrogenated components would be the determination of the charge-charge structure factor or of the related static dielectric function.

7.2 IN10 AND IN11 DYNAMICS. — The slow mode was observed with  $PSS_H Na$  on IN11, in the  $q$  range  $0.2 \text{ nm}^{-1} < q < 2.7 \text{ nm}^{-1}$ . The measurements made with  $PSS_H TMA_D$  and  $PSS_H TMA_D$  on IN10 are inconclusive in the lower  $q$  range (up to  $1.5 \text{ nm}^{-1}$ ), but we observe one and the same mode with the two samples for the larger  $q$  values. (Within the experimental and numerical (deconvolution) errors). The dispersion relation of this mode meshes smoothly with the one obtained, at two  $q$  values, with  $PSS_H TMA_H$ , using the spin-echo spectrometer. Keeping in mind that IN11 can only « see » the slowest mode of a system, we draw the conclusion that we

also observed the slow mode with the IN10 experimental design. Thus the gathered informations about this slow mode cover a rather wide range of reciprocal space :  $0.2 \text{ nm}^{-1} < q < 3.1 \text{ nm}^{-1}$ . We summarize here the results obtained with IN11 (§ 5.2.1) and with IN10 (§ 5.2.2). The effective diffusion coefficient defined from the slow mode relaxation frequency is at first a rapidly decreasing function of  $q$  and then, after a transition zone near  $q_m$ , becomes a constant. (The last point on figure 5 (for  $\text{PSS}_H\text{Na}$ ) is a long way out, but the IN10 measurements, (for the  $\text{PSSTMA}$ 's) with larger  $q$ 's, ascertain that  $D_{\text{eff}}(q)$  becomes actually constant.) This behaviour agrees rather well with the predictions about  $D(q)$  of reference [5], and is certainly not incompatible with the ones arising from the multicomponent dynamical analysis. The latter, valid in the small- $q$  limit, might still be applicable to the very first  $q$  values scanned, and it indeed predicts a large diffusion coefficient, decreasing as  $q$  increases because of the decoupling that gradually occurs between counterions and polyions. Of course, much stronger evidence for the counterion-polyion coupling would be the experimental determination of the « plasmon » mode.

The behaviour of the polyion diffusion coefficient at large  $q$  is easily understood on the basis of an analogy between neutral and charged polymer structure. The neutral polymer chain is flexible at all scales (down to the small monomer size). The size of moving elements probed at the wavevector  $q$  is of the order of  $q^{-1}$ , and an elementary application of the Stokes-Einstein law gives a diffusion coefficient increasing linearly with  $q$ , as is actually observed [19]. The charged polymer chain is also flexible, but only down to its (large) persistence length  $l_p$ . The size of moving elements probed at wavevector  $q > l_p^{-1}$  is always  $l_p$  and thus the diffusion coefficient is constant.

It is also of interest to extract from our results the mobility  $\mu(q)$ , since such a quantity is theoretically important. We define  $\mu(q)$  here as  $\mu(q) \propto D_{\text{eff}}(q) S_{11}(q)$  using our experimental  $D_{\text{eff}}$  and  $S_{11}$ . The resulting curve is plotted in figure 10. Because of the lack of precision, a precise, quantitative law cannot be derived

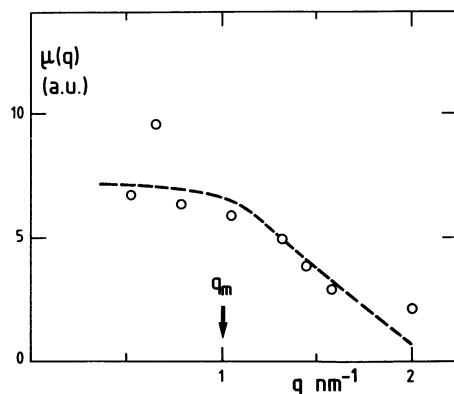


Fig. 10. — Mobility  $\mu(q)$  ( $\text{PSS}_H\text{Na}$  sample). The dashed line is only an eye guide.

from our data. Nevertheless it seems probable that the behaviour of  $\mu$  changes near  $q_m$ , and this is in conflict with the predictions of reference [5], which indeed give two different behaviours ( $\mu$  constant and then  $\mu$  decreasing as  $q^{-1}$ ), but with a transition zone located at  $q \sim l_p^{-1}$  instead of  $q \sim q_m$ .

The conclusions of this discussion about the slow mode are the following :

As hinted in the previous study [5], the slow mode diffusion coefficient, after a sharp decrease, becomes a constant when  $q$  increases beyond  $q_m$ . This behaviour at large  $q$  may be simply understood in terms of a large persistence length associated with the charged chain, but its interpretation using a rod-like mobility is perhaps questionable, because it rests on a very crude model for the structure of the polyelectrolyte chain.

The coupling between counterions and polyions is not evident in the  $q$  range of our study of the slow mode.

We still have to discuss our failure to observe the « plasmon » mode. The experiments performed with IN10, which probes faster relaxation phenomena than IN11, were originally designed to point out the two-mode decomposition of the coherent contribution to the total scattered intensity, and to study the dispersion relation of the faster mode. The « plasmon » mode is most easily observed when the slow mode amplitude  $S(q)$  is zero; then :

$$I(q, t) = \mathcal{F}(q) e^{-t/\tau}.$$

The condition  $S(q) = 0$  may in principle be obtained by a good choice of the coherent scattering lengths, or of the contrast lengths, and this is easily done by labelling either the sample or the solvent. Incidentally, this justifies the use of neutron scattering methods, though the « plasmon » behaviour is a small  $q$  property, *a priori* better suited to light-scattering methods. In practice, because of the apparatus limits, we were probably at all times out of the proper  $q$  range to observe coupled-ion dynamics. Moreover, our choice for labelling the samples appears to have been inadequate : the  $\text{PSS}_D\text{TMA}_D$  sample is not luminous enough; the  $\text{PSS}_D\text{TMA}_H$  sample is mostly an *incoherent* scatterer. (Parenthetically, we thus observed the counterion self diffusion motion, which, at the space-time scales probed, remains purely Brownian in spite of electrical interactions and possible exchange kinetic between « free » and « condensed » counterions). Our best samples,  $\text{PSS}_H\text{TMA}_D$  and  $\text{PSS}_H\text{TMA}_H$ , both have an important coherent contribution but, unfortunately, no two-mode superposition could be clearly evidenced, and the only well-defined mode seen is the slow mode !

**Acknowledgments.** — We thank M. Nierlich, J. P. Cotton and M. Daoud for their help in the experiment. We acknowledge fruitful discussions with F. Brochard, P. G. de Gennes and G. Weill.

## APPENDIX A

The dynamic matrix  $A(\mathbf{q})$  is :  $A(\mathbf{q}) = \begin{bmatrix} A_{11} & A_{12} \\ A_{21} & A_{22} \end{bmatrix}$ .

Its eigenvalues are :

$$\lambda = \frac{1}{2}[A_{11} + A_{22} + \sqrt{(A_{11} - A_{22})^2 + 4 A_{12} A_{21}}]$$

$$\mu = \frac{1}{2}[A_{11} + A_{22} - \sqrt{(A_{11} - A_{22})^2 + 4 A_{12} A_{21}}].$$

We assume that they are real and negative. These eigenvalues are related to the relaxation frequencies  $\tau_r^{-1}$  and  $\tau_s^{-1}$  :  $\tau_r^{-1} = -\mu$ ;  $\tau_s^{-1} = -\lambda$ . The matrix  $e^{A(\mathbf{q})t}$  is then :

$$e^{A(\mathbf{q})t} = \frac{1}{\mu - \lambda} \left\{ \begin{bmatrix} \mu - A_{11} & -A_{12} \\ -A_{21} & -(\lambda - A_{11}) \end{bmatrix} e^{\lambda t} + \begin{bmatrix} -(\lambda - A_{11}) & A_{12} \\ A_{21} & \mu - A_{11} \end{bmatrix} e^{\mu t} \right\}.$$

With this expression, the calculation of  $I(\mathbf{q}, t) = B^+ Q B$  is straight-forward :  $I(\mathbf{q}, t) = S(\mathbf{q}) e^{\lambda t} + \mathcal{F}(\mathbf{q}) e^{\mu t}$ , with :

$$S(\mathbf{q}) = \frac{1}{\mu - \lambda} [(b_1^2(\mu - A_{11}) - b_1 b_2 A_{21}) S_{11}(\mathbf{q}) - (b_1^2 A_{12} + b_2^2 A_{21} - b_1 b_2(\mu - \lambda)) S_{12}(\mathbf{q}) - (b_2^2(\lambda - A_{11}) + b_1 b_2 A_{12}) S_{22}(\mathbf{q})]$$

$$\mathcal{F}(\mathbf{q}) = \frac{1}{\mu - \lambda} [- (b_1^2(\lambda - A_{11}) - b_1 b_2 A_{21}) S_{11}(\mathbf{q}) + (b_1^2 A_{12} + b_2^2 A_{21} + b_1 b_2(\mu - \lambda)) S_{12}(\mathbf{q}) + (b_2^2(\mu - A_{11}) + b_1 b_2 A_{12}) S_{22}(\mathbf{q})]$$

or, equivalently,  $\mathcal{F}(\mathbf{q}) = -S(\mathbf{q}) + b_1^2 S_{11}(\mathbf{q}) + 2 b_1 b_2 S_{12}(\mathbf{q}) + b_2^2 S_{22}(\mathbf{q})$ .

## APPENDIX B

**The electroneutrality relations.** — We consider a multicomponent system with component  $I$  bearing the electric charge  $Z_I$ .

The number fraction of component  $I$  is  $x_I$ , the total number of particles,  $N$ , and the volume,  $V$ .

We now ask for the mean electric charge  $Q_I(\mathbf{r})$  around a particle at position  $\mathbf{r}$  belonging to component  $I$ . We have

$$Q_I(\mathbf{r}) = \sum_J Z_J p_{IJ}(\mathbf{r})$$

where  $p_{IJ}$  is the probability of finding a  $J$ -particle somewhere when there is a  $I$ -particle at  $\mathbf{r}$ ; therefore

$$p_{IJ}(\mathbf{r}) = \int \sum_{i=1}^{x_J N} p_{IJ}^{(i)}(\mathbf{r} | \mathbf{r}') d^3 r',$$

$p_{IJ}^{(i)}(\mathbf{r} | \mathbf{r}')$  being the conditional probability of finding the  $i$ th  $J$ -particle at  $\mathbf{r}'$  with a  $I$ -particle at  $\mathbf{r}$ . It is related to the pair-correlation function  $g_{IJ}$  through :

$$P_{IJ}^{(i)}(\mathbf{r} | \mathbf{r}') = \frac{1}{V} (1 + g_{IJ}(|\mathbf{r} - \mathbf{r}'|)).$$

Thus

$$Q_I(\mathbf{r}) = \sum_J Z_J x_J \frac{N}{V} \left[ V + \int g_{IJ}(|\mathbf{u}|) d^3 u \right]$$

or, using the global electroneutrality relation

$$\sum_J x_J Z_J = 0, \quad Q_I(\mathbf{r}) = \frac{N}{V} \sum_J Z_J x_J \int g_{IJ}(|\mathbf{u}|) d^3 u.$$

The total electric charge of the system is equal to the sum of the charge  $Z_I$  of any  $I$ -particle at some position  $\mathbf{r}$  and the charge  $Q_I(\mathbf{r})$  of all the other particles surrounding this one. This total charge is zero; thus

$$Z_I + Q_I(\mathbf{r}) = 0. \quad (\text{B1})$$

We now consider the partial  $I - J$  coherent static scattering function  $S_{IJ}(\mathbf{q})$ , defined in Part 2. We have

$$S_{IJ}(\mathbf{q}) = N \left[ x_I \delta_{IJ} + \frac{N}{V} x_I x_J \int e^{i\mathbf{q}\cdot\mathbf{r}} (1 + g_{IJ}(|\mathbf{r}|)) d^3r \right]$$

or

$$S_{IJ}(\mathbf{q}) = N \left[ x_I \delta_{IJ} + N x_I x_J \delta_{q,0} + \frac{N}{V} x_I x_J \int e^{i\mathbf{q}\cdot\mathbf{r}} g_{IJ}(|\mathbf{r}|) d^3r \right].$$

Thus

$$\sum_J Z_J x_J \frac{N}{V} \int g_{IJ}(|\mathbf{r}|) d^3r = \lim_{q \rightarrow 0^+} \sum_J \left( \frac{S_{IJ}(\mathbf{q})}{N x_I} - \delta_{IJ} \right) Z_J$$

or

$$Q_I = -Z_I + \frac{1}{N x_I} \sum_J S_{IJ}(0_+) Z_J.$$

With the electroneutrality relation (B1), we finally arrive at :

$$\sum_J Z_J S_{IJ}(0_+) = 0.$$

In our case,  $Z_0 = 0$ ,  $Z_1 = -ze$ ,  $Z_2 = +e$  :

$$zS_{11}(0_+) = S_{12}(0_+) \quad \text{and} \quad zS_{12}(0_+) = S_{22}(0_+)$$

(since  $S_{IJ} = S_{JI}$ ).

#### References

- [1] PHILLIES, G. D. J., *J. Chem. Phys.* **60** (1974) 983.  
 [2] BERNE and PECORA, *Dynamic. Light Scattering*, Chap. 9 (J. Wiley, New York).  
 [3] NIERLICH, M., WILLIAMS, C. E., BOUÉ, F., COTTON, J. P., DAUD, M., FARNOUX, B., JANNINK, G., PICOT, C., MOAN, M., WOLFF, C., RINAUDO, M., de GENNES, P. G., *J. Physique* **40** (1979) 701.  
 [4] Anomalous as referred to the Nernst-Einstein law; see e.g. HANSEN, J. P., MACDONALD, I. R., *Phys. Rev.* **23** (1981) 2041.  
 [5] HAYTER, J. B., JANNINK, G., BROCHARD-WYART, F., de GENNES, P. G., *J. Physique-Lett.* **41** (1980) L-451.  
 [6] VAN HOVE, L., *Phys. Rev.* **95** (1954) 249.  
 [7] VINK, H., *Makromol. Chem.* **182** (1981) 279.  
 [8] TONDRE, C., ZANA, R., *J. Phys. Chem.* **76** (1972) 3451.  
 [9] STABINGER, H., LEOPOLD, H., KRATKY, O., *Digital densitometer for liquids and gases* (Anton Paar Gaz Austria) 1966.  
 [10] MEZEL, F., *Z. Phys.* **255** (1972) 146.  
 [11] HAYTER, J. B., *Z. Phys.* **B 31** (1978) 117.  
 [12] HAYTER, J. B., ILL Internal Scientific Report 78HA50 (Grenoble).  
 [13] MANNING, G. S., *J. Chem. Phys.* **51** (1969) 934.  
 [14] MANNING, G. S., *J. Chem. Phys.* **51** (1969) 924.  
 [15] As obtained from equivalent conductivity measurements, and using the Nernst-Einstein law. *Electrolyte Solutions*, ROBINSON, R. A. and STOKES, R. H. (Butterworths, London) 1970.  
 [16] OKUBO, T., ISE, N., *Macromolecules* **2** (1969) 407.  
 [17] DAUD, M., COTTON, J. P., FARNOUX, B., JANNINK, G., SARMA, G., BENOIT, H., DUPLESSIX, R., PICOT, C., de GENNES, P. G., *Macromolecules* **8** (1975) 804.  
 [18] DE GENNES, P. G., *Macromolecules* **9** (1976) 587.  
 [19] ADAM, M., DELSANTI, M., *Macromolecules* **10** (1977) 1229.  
 [20] ODIJK, T., HOUWAART, A. C., *J. Polym. Sci. Polym. Phys. Ed.* **16** (1978) 627.  
 [21] KUBO, R., *Rep. Prog. Phys.* **29** (1966) 255.